Journal of Cellular Biochemistry 96:1095–1109 (2005)

FAST TRACK

Cellular Localization of Human Rad51C and Regulation of Ubiquitin-Mediated Proteolysis of Rad51

Brian T. Bennett and Kendall L. Knight*

Department of Biochemistry and Molecular Pharmacology, University of Massachusetts Medical School, Aaron Lazare Medical Research Building, 364 Plantation Street, Worcester, Massachusetts 01605-2324

Abstract Rad51-catalyzed homologous recombination is an important pathway for repair of DNA double strand breaks and maintenance of genome integrity in vertebrate cells. Five proteins referred to as Rad51 paralogs promote Rad51 activity and are proposed to act at various, and in some cases, multiple stages in the recombination pathway. Imaging studies of native Rad51 have revealed its cellular response to DNA damage, yet visualization of the paralog proteins has met with limited success. In this study, we are able to detect endogenous Rad51C and Xrcc3 in human cells. In an effort to determine how Rad51, Rad51C, and Xrcc3 influence the pattern of localization of each other over the time course of DNA damage and repair, we have made the unexpected observation that Rad51 degradation via the ubiquitin-mediated proteasome pathway occurs as a natural part of recombinational DNA repair. Additionally, we find that Rad51C plays an important role in regulating this process. This article contains supplementary material, which may be viewed at the Journal of Cellular Biochemistry website at http://www.interscience.wiley.com/jpages/0730-2312/suppmat/index.html. J. Cell. Biochem. 96: 1095–1109, 2005.

Key words: human Rad51; human Rad51C; human Xrcc3; Rad51 ubiquitination; DNA double strand break repair; homologous recombination

Repair of DNA double strand breaks (DSBs) resulting from either endogenous sources, for example, errors in DNA replication, or following exposure to exogenous mutagens is critical for cell survival and the maintenance of genome integrity. Homologous recombination (HR) is an important pathway in mammalian cells for DSB repair [Pierce et al., 1999; Johnson and Jasin, 2000; Thompson and Schild, 2001]. The Rad51 protein provides the central activity in this pathway by catalyzing formation of crossover structures (Holliday junctions) between damaged DNA and an undamaged homologous chromosome, most frequently a sister chromatid [Sung et al., 2003; West, 2003]. A group of five Rad51-like proteins (Rad51 paralogs; Rad51B/L1, Rad51C/L2, Rad51D/L3, Xrcc2, and Xrcc3), originally identified in complementation screens and by sequence alignment with Rad51 [Albala et al., 1997; Tambini et al., 1997; Cartwright et al., 1998a,b; Dosanjh et al., 1998; Liu et al., 1998], have been shown to play important roles in supporting Rad51 function. Vertebrate cells deficient for any of the five paralogs show increased sensitivity to DNA damaging agents and increased levels of chromosomal abnormalities [Tebbs et al., 1995; Liu et al., 1998; Thacker, 1999; Sonoda et al., 2001; Takata et al., 2001; Thompson and Schild, 2001; Yoshihara et al., 2004]. Suppression of these defects is best achieved by transfection of the specific gene itself and not by over expression of RAD51 or other paralog genes [Takata et al., 2001; French et al., 2002], thus providing evidence that each paralog has an important, non-redundant function in HR. In response to DNA damage, the Rad51 protein forms distinct nuclear foci that appear to associate with DNA breaks [Haaf et al., 1999; Tashiro et al., 2000; Aten et al., 2004]. Each of the five paralog

Grant sponsor: D.O.D. Breast Cancer Research Program; Grant sponsor: NIH; Grant numbers: GM44772, GM65851.

*Correspondence to: Kendall L. Knight, Department of Biochemistry and Molecular Pharmacology, University of Massachusetts Medical School, Aaron Lazare Medical Research Building, 364 Plantation Street, Worcester, MA 01605-2324. E-mail: kendall.knight@umassmed.edu

Received 18 July 2005; Accepted 19 July 2005

DOI 10.1002/jcb.20640

proteins is required for DNA damage-induced nuclear Rad51 focus formation, demonstrating a likely role early in the HR pathway [Bishop et al., 1998; Takata et al., 2001; Yoshihara et al., 2004]. Additional evidence supports other roles for the paralog proteins at different points in the HR pathway. For example, defective processing of recombination intermediates is observed in both hamster and Arabidopsis XRCC3$^{-/-}$ cells [Brenneman et al., 2000; Bleuyard and White, 2004]. Additionally, recent studies show that Rad51C and Xrcc3 may play a direct role in Holliday junction resolution [Liu et al., 2004].

Specific protein–protein interactions between Rad51 paralog proteins have been demonstrated [Schild et al., 2000] and several complexes have been identified [Braybrooke et al., 2000; Kurumizaka et al., 2001; Masson et al., 2001a,b; Sigurdsson et al., 2001; Liu et al., 2002; Miller et al., 2002; Wiese et al., 2002]. It has been suggested that because Rad51C is present in three of the four complexes identified to date (BC, CX3, and BCDX2), it may play a more prominent role in regulating Rad51 and Rad51 paralog functions than other paralogs [French et al., 2003]. Additionally, Rad51C may be involved in trafficking recombination proteins to the nucleus [French et al., 2003]. Biochemical studies using purified paralog protein complexes have demonstrated DNA-dependent ATPase, DNA binding, substrate-specific strand transferase, and strand-separation activities [Thacker, 2005] but an integrated model of how these functions contribute to the HR pathway in the cell remains to be determined. Other than their requirement for the formation of DNA damage-induced Rad51 nuclear foci, little is currently known regarding specific cellular functions of the paralog proteins.

In this study, we use immunofluorescence imaging to show the cellular distribution of endogenous human Rad51C and Xrcc3 before DNA damage and over an extended time course of DNA damage and repair. The data show that both proteins localize to positions at the nuclear periphery and form distinct foci within the nucleus both before and after DNA damage. RNAi studies designed to understand the potential interdependence of the cellular localization of each protein have led us to discover a novel and unexpected function for Rad51C—regulation of ubiquitin-mediated degradation of Rad51.

MATERIALS AND METHODS

Cell Lines and Transfections

HEK293 cells were obtained from ATCC and were maintained in DMEM supplemented with 10% fetal bovine serum (FBS) and 1% Pen/Strep. In preparation for transfection, cells were maintained in DMEM plus 10% FBS. Transfection of specific siRNA duplexes (SMARTpool, Dharmacon) was performed using a lipid transfection method (Dharmafect, Dharmacon). A control siRNA against lamin A/C and a 3′-fluorescein labeled control siRNA with no matches in human genome (Qiagen, cat no. 1022079) showed no effect on Rad51, Rad51C, or Xrcc3 focus formation or protein levels as determined by Western blots (data not shown). Epoxomicin, a specific proteasome inhibitor (Sigma) was added at a final concentration of 5 μM to cells 1 h prior to exposure of cells to ionizing radiation (IR) for immunoprecipitation experiments (see below).

Antibodies

Primary antibodies were mouse monoclonal anti-phospho-histone H2AX biotin conjugate (clone JBW301, Upstate Biotechnology), mouse monoclonal anti-Rad51 (clone 3C10, Upstate Biotechnology), mouse monoclonal anti-Rad51C (clone 2H11/6, Novus Biologicals, Inc.), mouse monoclonal anti-Xrcc3 (10F1/6, Novus Biologicals, Inc.) and all were diluted 1:500 for immunofluorescence studies. Monoclonal Rad51C and Xrcc3 antibodies were protein-A purified. Alexa647 streptavidin conjugate and Alexa488 secondary antibodies (Molecular Probes) were diluted 1:1,000. All dilutions were in PBS containing 20% marine blocking agent (East Coast Biologicals, Inc.). DNA was counterstained with Vectashield Fluorescent Mounting Media containing DAPI (4′, 6′-diamidino-2-phenylindole; Vector Laboratories). Antibodies used for immunofluorescence were the same used for Western blots and immunoprecipitation experiments. Western blot analysis for ubiquitin was performed using rabbit polyclonal anti-ubiquitin (Upstate Biotechnologies) at a 1:500 dilution.

Immunostaining and Confocal Microscopy

Cells were grown on coverslips in a 6 well dish. For fixation, media was aspirated off and cells were washed once with PBS and immersed in 100% methanol at −20°C for 8 min. Cells were

blocked in a marine blocking agent overnight at 4°C. Incubation with primary and secondary antibodies was performed in 6 well dishes for 1 h at 37°C in a humid environment using a slide warmer (Fisher). For all double staining procedures, cells were stained in sequential fashion as opposed to using mixes of antibodies. For example, cells were incubated first with the primary antibody directed against Rad51, Rad51C, or Xrcc3 followed by incubation with the secondary Alexa488. Subsequently, cells were incubated with anti-γH2AX biotin conjugate primary antibody followed by the secondary Alexa647 streptavidin conjugate. Cells were washed five times for 5 min each in PBS after incubation with both primary and secondary antibodies. Coverslips were mounted using Vectashield with DAPI and sealed with polyurethane (nail polish) then stored in the dark at 4°C. Visualization of immunostains was performed by confocal microscopy using a Leica TCS SP2 AOBS instrument and image processing was performed using the accompanying Leica Confocal Software TCS SP2. Microscope settings are identical for all images shown. Additionally, all images were corrected to the same values using Leica software. Images were processed and are presented in CMYK colors to avoid loss of resolution during the RGB to CMYK transition.

Damage-Induced DNA Double Strand Breaks

Cells were exposed to 8 Gy ionizing radiation (^{137}Cs) using a Gammacell 40 (MDS Nordion Ottawa, ON, Canada). After exposure cells were allowed to recover at 37°C (5% CO_2) for the indicated times. Cells were then methanol fixed and prepared for immunostaining.

Western Blotting

HEK293 cells were transfected with the appropriate siRNA as indicated. Cells were harvested 48 h post transfection washed with PBS and lysed with RIPA buffer (25 mM Tris pH 7.4, 0.5% Triton X-100, 0.5% sodium deoxycholate, 0.05% sodium dodecyl sulfate, 0.05 mM EDTA pH 7.0, 75 mM NaCl) and total protein was determined with BCA Protein Assay Kit (Pierce). Acrylamide mini-gels (10%) were run with 60 μg of total protein in each lane and transferred to PVDF membranes using a semi-dry procedure (Bio-rad) at 20 V for 20 min. Membranes were incubated in blocking buffer (10 mM Tris-HCl pH 8.0, 300 mM NaCl, 0.025% Tween 20) containing 15% instant nonfat dry milk for 45 min. Primary antibodies were added (1:1,000) in blocking buffer containing 2% instant nonfat dry milk for 1 h and membranes were washed five times for 5 min each in blocking buffer. Mouse anti-α-tubulin (TU-02, Santa Cruz Biotechnology) was diluted 1:10,000. Peroxidase conjugated anti-mouse and anti-rabbit secondary antibodies (Visualizer, Upstate) were added (1:12,000) for 45 min and membranes washed as above. Membranes were incubated with the appropriate chemiluminescent detection reagent for 10–60 s, exposed to X-ray film and developed (Kodak 2000A XOMAT processor). To detect ubiquitinated Rad51, blots that had been stained for Rad51 were incubated in stripping buffer (62.5 mM Tris-HCl, pH 6.0, 2% SDS, 100 mM βME) at 50°C for 30 min, washed twice for 20 min with blocking buffer and stained as above using anti-ubiquitin antibodies.

Immunoprecipitation

Cells were harvested and treated with lysis buffer (20 mM Tris, pH 8.0, 150 mM NaCl, 1 mM EDTA, 0.5% NP-40, 1 mM phenylmethylsulfonyl fluoride, leupeptin (10 μg/ml), aprotinin (10 μg/ml)) for 30 min at 4°C. Extracts were clarified by centrifugation for 10 min at 12,500*g*. The supernatant was incubated with anti-Rad51 (see above) and 30 μl protein A beads (Amersham) for 2 h at 4°C and washed three times using the following buffer (20 mM Tris (pH 8.0), 150 mM NaCl, 1 mM EDTA, 0.5% NP-40). Beads were boiled in SDS loading buffer and proteins were analyzed by Western blots as described above.

RESULTS

Cellular Localization of Rad51, Rad51C, and Xrcc3 Prior to DNA Damage and Throughout a Time Course of DNA Damage and Repair

To detect the cellular localization of endogenous Rad51, Rad51C, and Xrcc3 proteins, HEK293 cells were fixed and stained for each protein prior to damage and at t = 0.5, 1, 2, 4, 6, and 8 h following exposure to ionizing radiation (IR, 8 Gy). We followed the staining of γH2AX as a marker for DNA double-strand breaks [Rogakou et al., 1998]. At t = 0, only minor background γH2AX staining is observed (Figs. 1 and 3). At t = 0.5 h there is a dramatic increase

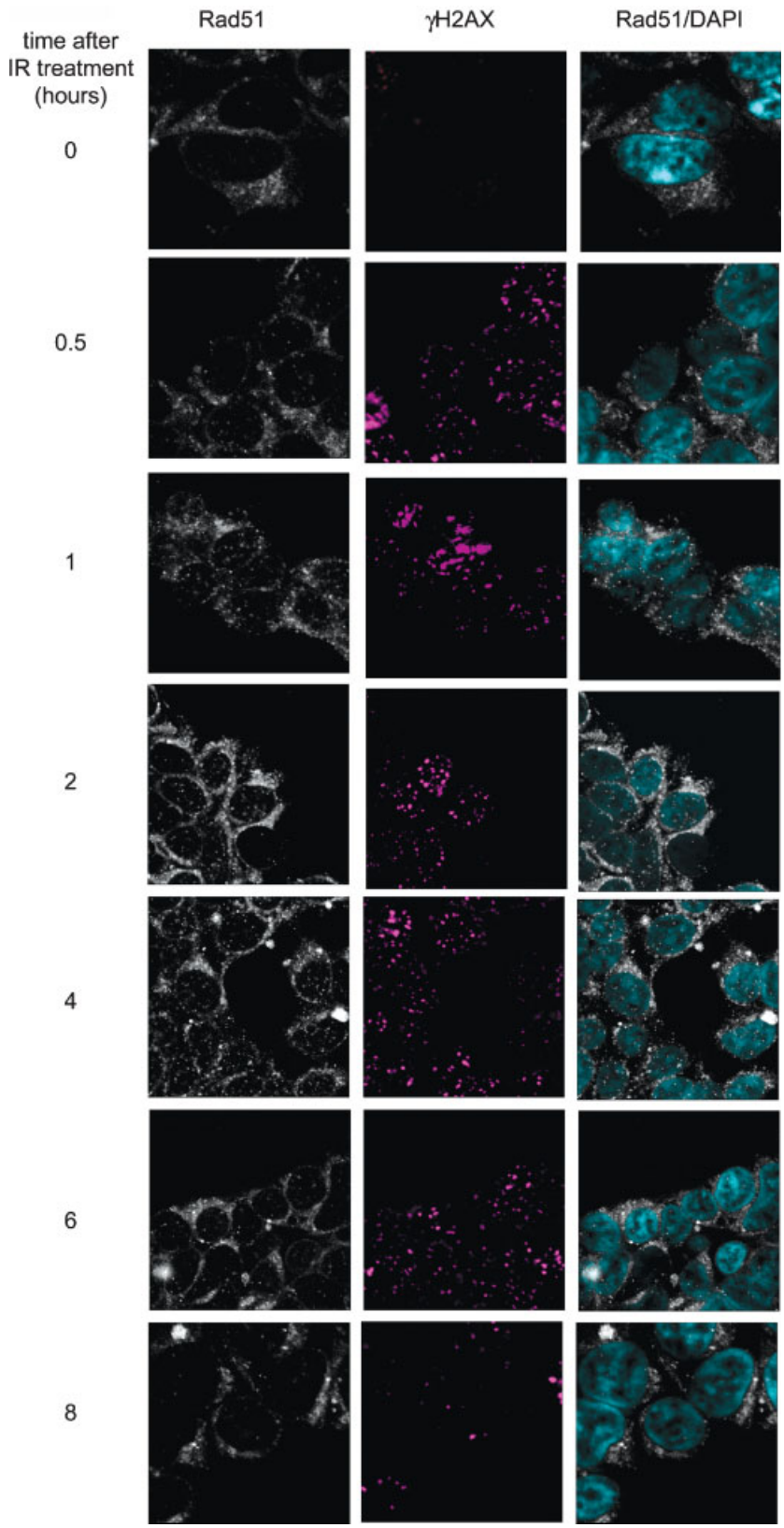

Fig. 1. Ionizing radiation-induced nuclear Rad51 foci form early following DNA damage and disassemble over an 8 h time course of DNA repair. HEK293 cells were stained with anti-Rad51 (gray), anti-γH2AX (magenta), and DAPI (cyan) at the indicated times before and after exposure to ionizing radiation (8 Gy).

in the appearance of nuclear γH2AX. This persists for 6 h and diminishes at t = 8 h, indicative of repair of DSBs.

For Rad51, we find that prior to DNA damage protein staining appears in the cytoplasm, and there are occasional nuclear foci (Fig. 1). These have been previously described as S-phase foci [Chen et al., 1998, 1999; Tarsounas et al., 2004]. Significant levels of cytoplasmic Rad51 have also been observed by Western analysis of subcellular fractions [Yoshikawa et al., 2000; Davies et al., 2001]. At t = 0.5 h, there is a distinct increase in the number of nuclear foci, and as time progresses the number and size of these foci peak between 2 and 4 h. At t = 6 h the number of nuclear Rad51 foci is noticeably diminished, and at 8 h the staining appears similar to that seen at t = 0 (Fig. 1 and Supplementary Material can be found online at http://www.interscience.wiley.com/jpages/0730-2312/suppmat/index.html). We note also that while cytoplasmic staining of Rad51 is somewhat diffuse at t = 0, 0.5, and 1 h following exposure to IR, at 2 and 4 h Rad51 cytoplasmic staining is concentrated more at the nuclear periphery, and returns to a more diffuse appearance at t = 8 h. For all time points, >90% of the cell population showed similar staining patterns.

In contrast to Rad51, staining for endogenous Rad51C revealed an unexpected pattern in that distinct nuclear foci were present in all cells prior to DNA damage (Fig. 2). As for Rad51, Rad51C also appears to concentrate at the nuclear periphery following DNA damage. While this perinuclear staining pattern appears slightly more diffuse at t = 0 and 0.5 h relative to its more distinct appearance throughout the remainder of the time course, judging from the entire field of cells it is difficult to say to what extent this is a DNA damaged-induced phenomenon. However, it is clear from the data in Figures 1 and 2 that while the staining pattern of Rad51 shows a significant response to DNA damage and repair, especially with regard to nuclear focus formation, changes in the cellular staining pattern of Rad51C are more subtle. For all time points the number of cells containing Rad51C foci both before and after DNA damage was >90%. Our observation of endogenous Rad51C in both the cytoplasm and nucleus is supported by previous studies in which endogenous human Rad51C was shown to exist in both cellular compartments using Western blot analysis of subcellular fractions [Miller et al., 2005].

The cellular appearance of endogenous Xrcc3 is similar to that observed for Rad51C (Fig. 3). Staining of Xrcc3 shows distinct nuclear foci prior to DNA damage [Forget et al., 2004] as well as clusters of protein in the cytoplasm and perinuclear region (Fig. 3). At 6 and 8 h following exposure to IR, the number of nuclear Xrcc3 foci appear to diminish, but as for Rad51C this change is significantly more subtle than that observed for Rad51 (Fig. 1). Also, perinuclear clustering of Xrcc3 appears more concentrated following DNA damage (for example, see Fig. 3, t = 4 h) as compared to a more diffuse staining at t = 0. Similar to Figures 1 and 2, >90% of the cells at each time point showed similar staining patterns. The fact that the cellular staining pattern of Xrcc3 mimics that of Rad51C supports the observation that these two proteins can exist as a stable heterodimer [Kurumizaka et al., 2001; Masson et al., 2001a; Wiese et al., 2002]. The primary antibodies used to stain both Rad51C and Xrcc3 are mouse monoclonals of the same iso-type, which prevents co-localization studies, but methods to achieve this are currently under development. Formation of DNA damage-induced nuclear Rad51 foci requires Xrcc3 as well as Rad51C and we now observe both Xrcc3 and Rad51C in nuclear foci prior to DNA damage. Whether these foci are centers at which Rad51C and Xrcc3 function, or serve to sequester both proteins for release during DNA repair remains to be determined (see Discussion).

Validation of Antibody Specificity

Prior use of the unpurified anti-Rad51C and Xrcc3 monoclonal antibodies on HEK293 and HeLa whole cell extracts revealed multiple bands in Western blots, thereby precluding their use in immunofluorescence studies (data not shown). However, we purified the anti-Xrcc3 monoclonal using a protein-A Sepharose procedure (http://www.novus-biologicals.com/data_sheet.php/81/S/xrcc3/0) and have been able to successfully use this antibody in immunofluorescence studies (Forget et al., 2004). In the present study, monoclonal antibodies against Rad51C and Xrcc3 obtained from Novus Biologicals, Inc., were protein-A purified. To demonstrate that the staining patterns observed in Figures 1, 2, and 3 are specific to

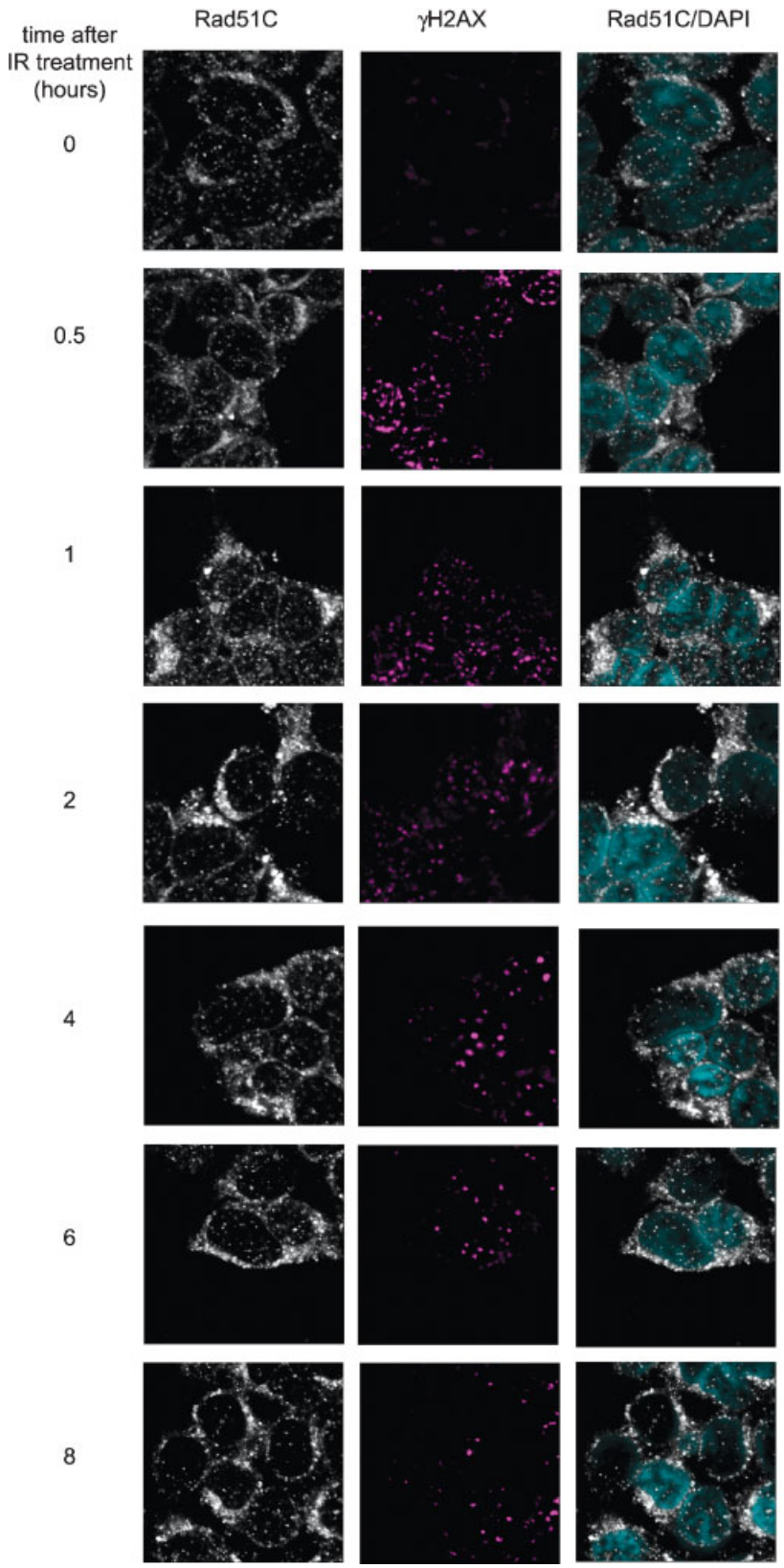

Fig. 2. Rad51C forms distinct nuclear foci prior to DNA damage that persist throughout the time course of DNA repair. HEK293 cells were stained with anti-Rad51C (gray), anti-γH2AX (magenta), and DAPI (cyan) at the indicated times before and after exposure to ionizing radiation (8 Gy).

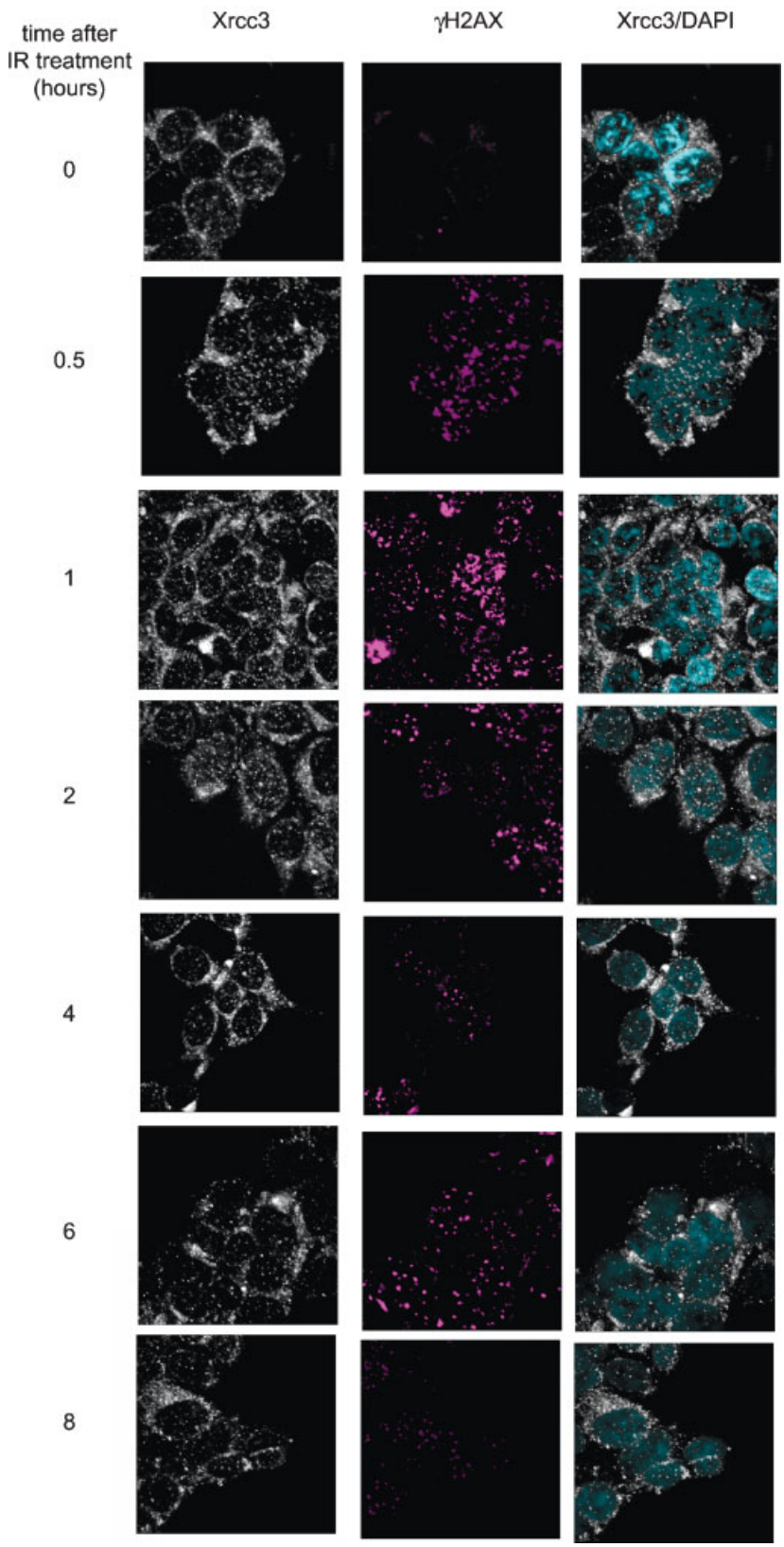

Fig. 3. Nuclear Xrcc3 foci are present at all times before and after exposure of cells to ionizing radiation. HEK293 cells were stained with anti-Xrcc3 (gray), anti-γH2AX (magenta), and DAPI (cyan) at the indicated times before and after exposure to ionizing radiation (8 Gy).

the proteins of interest, we analyzed immunofluorescence images of cells treated with small interfering RNAs (siRNAs). HEK293 cells were transfected with siRNAs specific to Rad51, Rad51C, or Xrcc3 and exposed to IR (8 Gy) 48 h later. Two hours following IR treatment, cells were fixed and stained using the procedure identical to that used in Figures 1, 2, and 3. We find that in each case the signal for Rad51, Rad51C, and Xrcc3 is almost completely eliminated by its specific siRNA (Fig. 4A). A low level, residual staining can in part be explained by the slight background contributed by the AlexaFluor488 secondary antibody (Fig. 4B). The fact that staining with DAPI and anti-γH2AX is localized exclusively to the nucleus precludes the possibility that cytoplasmic and perinuclear staining of Rad51, Rad51C, and Xrcc3 result from disruption of the nuclear membrane during fixation. Again, our observations are supported by previous studies of various human cell types, for example, pancreatic and breast epithelial cells, which show a significant amount of cytoplasmic Rad51 [Yoshikawa et al., 2000; Davies et al., 2001], and HeLa cells showing cytoplasmic Rad51C [Miller et al., 2005].

The specificity of the primary antibodies, as well as the siRNAs, was further demonstrated by Western blot analysis of whole cell extracts. The data show that siRNAs directed against Rad51, Rad51C, or Xrcc3 specifically reduce the amount of each protein by = 95% (Fig. 4C,D). Coomassie-stained gels show a large number of bands both above and below the position of each protein of interest (not shown), yet the purified

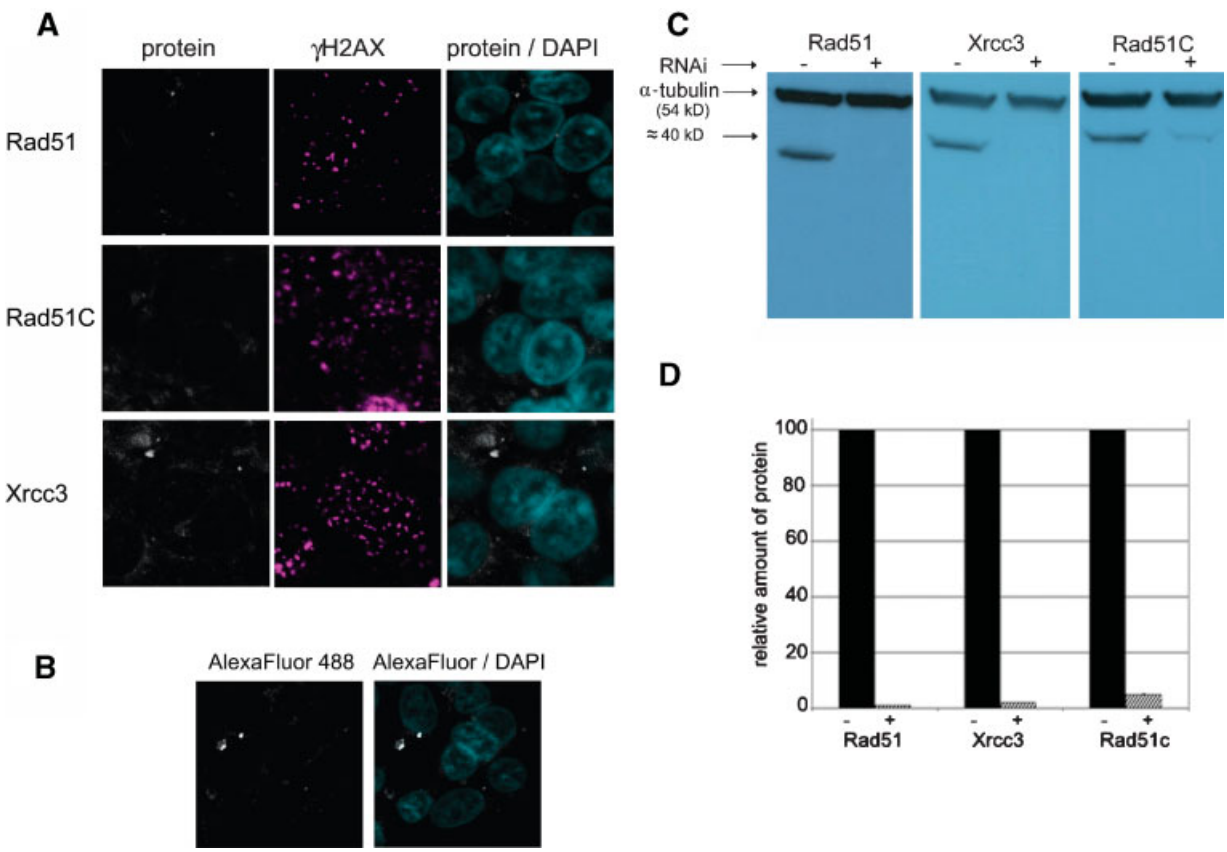

Fig. 4. Antibodies and siRNAs are specific to the designated protein. **A**: Cells were stained with antibodies against the indicated protein (gray), anti-γH2AX (magenta), and DAPI (cyan) 2 h following exposure to ionizing radiation (8 Gy). **B**: Cells were stained only with DAPI (cyan) and AlexaFluor488 secondary antibody (gray) that is used in all other immunofluorescence images to indicate the small background contribution made by this antibody. **C**: Western blots were performed using anti-Rad51, anti-Rad51C or anti-Xrcc3 on whole cell extracts from cells incubated with the indicated siRNAs. Protein molecular mass is from http://www.hprd.org/protein: Rad51 = 36,968 Da; Xrcc3 = 37,842; Rad51C = 42,192. **D**: Relative amounts of each protein following treatment with specific siRNAs were determined from scans of Western blots from three separate experiments.

primary antibodies directed against each protein reveal only that protein (Fig. 4C). No cross-reacting protein was visible in many repeated Western blots of HEK293 whole cell extracts using each of the primary antibodies against Rad51, Rad51C, and Xrcc3. Having established the specificity of both the siRNAs and the primary antibodies, we next performed experiments to determine the effect that knock down of each protein would have on the others.

Loss of Rad51C Results in Degradation of Rad51 Following DNA Damage

HEK293 cells transfected as above with siRNAs against Rad51, Rad51C, or Xrcc3 were exposed to 8 Gy IR and fixed 2 h later. As expected, treatment of cells with Rad51 specific siRNAs resulted in specific loss of Rad51 staining (Fig. 5A). We find that Rad51C staining is unaffected by Rad51 specific siRNAs, and in agreement with recent studies we find that this treatment results in no change in Xrcc3 staining [Forget et al., 2004], and (Fig. 5B,C, respectively). Therefore, while formation of DNA damage-induced Rad51 foci requires each of the five Rad51 paralog proteins [Bishop et al., 1998; Takata et al., 2001], formation of Rad51C and Xrcc3 foci does not require Rad51.

Cells treated with siRNAs against Rad51C showed the expected loss of Rad51C staining (Fig. 5E), and while the total amount of Xrcc3 staining in these cells appears somewhat reduced (Fig. 5F) relative to non-siRNA treated cells (Fig. 3), the general Xrcc3 staining pattern in the nucleus, cytoplasm and perinuclear region remained very similar to non-treated cells. Remarkably however, we observe that treatment of cells with Rad51C-specific siRNA results in a total loss of Rad51 staining (Fig. 5D). Given the data shown below, and the fact that all siRNAs used in this study had no significant sequence similarity, this effect did not result from direct knock down of Rad51 mRNA by Rad51C siRNA.

Cells treated with siRNAs against Xrcc3 showed the expected loss of Xrcc3 (Fig. 5I), as well as the expected inability to form DNA damage-induced nuclear Rad51 foci (Fig. 5G). However, cellular staining of Rad51 is still apparent, although it appears to be somewhat reduced relative to cells not treated with Xrcc3 siRNAs (Figs. 1 and 2 h panel). Staining of Rad51C (Fig. 5H) is similar to that seen in untreated cells (Fig. 2). Therefore, these data reveal an entirely unexpected result in that knock down of Rad51C appears to result in loss of Rad51 following DNA damage.

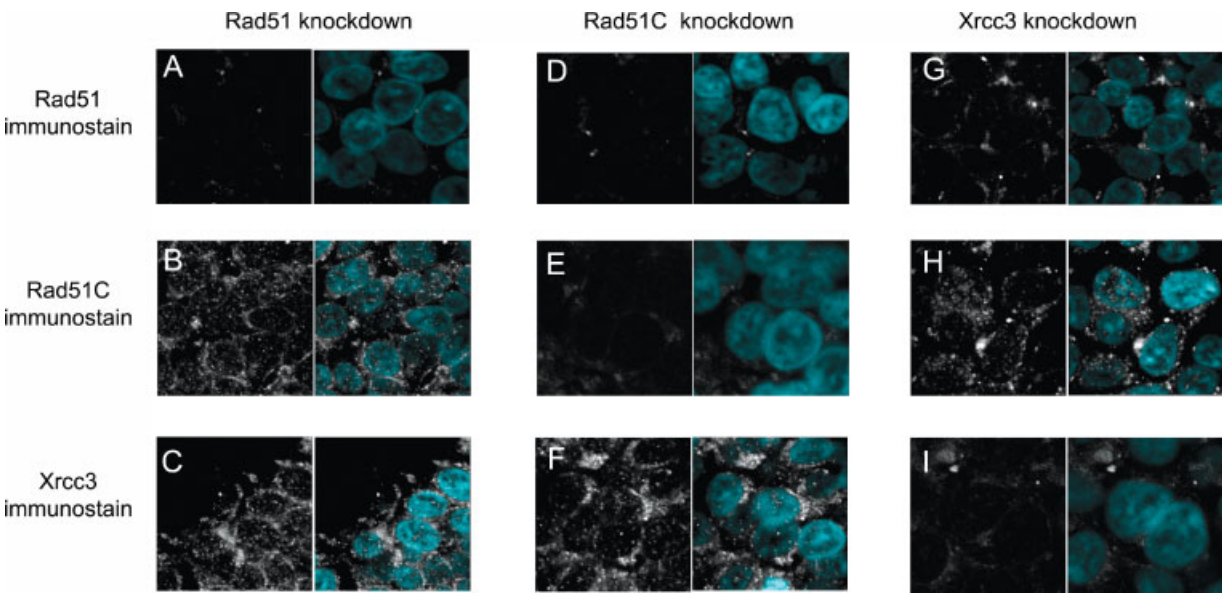

Fig. 5. Knockdown of Rad51C results in complete loss of Rad51 immunostaining following DNA damage. Cells were incubated with siRNAs directed against Rad51 (**A**–**C**), Rad51C (**D**–**F**), or Xrcc3 (**G**–**I**) for 46 h and then treated with ionizing radiation (8 Gy). Two hours following DNA damage cells were stained using anti-Rad51 (A, D, G), anti-Rad51C (B, E, H), or anti-Xrcc3 (C, F, I) and DAPI. The images in **panels A**, **E**, and **I** are the same as those shown in Figure 4A.

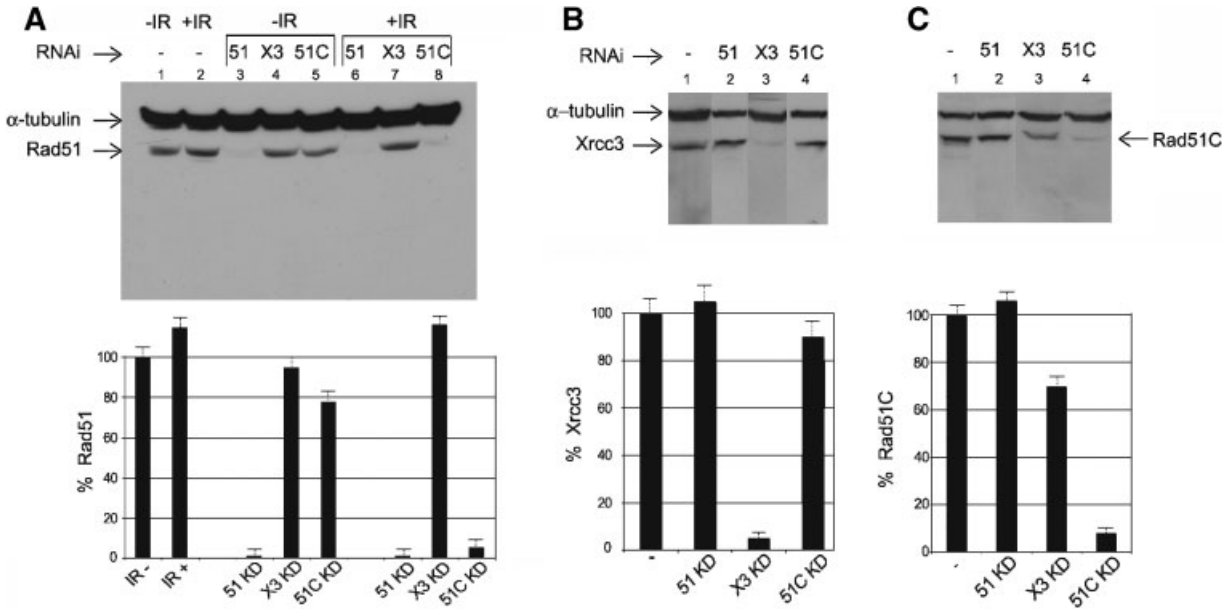

Fig. 6. Lack of Rad51C results in degradation of Rad51. **A**: Western blot developed with anti-Rad51 using whole cell extracts from cells treated with the indicated siRNAs 48 h prior to IR exposure. Extracts were obtained from cells that had not been exposed to DNA damage (−IR) or 2 h following exposure to 8 Gy ionizing radiation (+IR). **B**, **C**: Western blots developed with anti-Xrcc3 and anti-Rad51C, respectively. Whole cell extracts were obtained from cells treated with the indicated siRNAs for 48 h followed by exposure to ionizing radiation (8 Gy) and harvested 2 h later. Histograms accompanying each blot show relative amounts of each protein averaged over three separate experiments.

To further explore this idea, we performed Western blot analysis of HEK293 cells treated with siRNAs against each protein and compared the levels of each of the other proteins both before and 2 h after DNA damage (8 Gy, IR). In Figure 6A we show a Rad51 blot of extracts from cells treated with each siRNA. In control cells not treated with siRNA, there appears to be a slight increase in the total amount of Rad51 following IR exposure (lanes 1 and 2), consistent with a small cell cycle-dependent increase observed previously [Chen et al., 1997; Daboussi et al., 2002]. Cells treated with Rad51 siRNA show a specific loss of protein in the absence (lane 3) or presence (lane 6) of IR exposure. Cells treated with Xrcc3 siRNA show little effect on the total amount of Rad51 with or without DNA damage (lanes 4 and 7). In contrast, cells treated with Rad51C siRNA show nearly a complete loss of Rad51 following exposure to IR (lane 8) and what appears to be an approximate 20% decrease in Rad51 protein levels in the absence of IR exposure (lane 5). Previous studies [Lio et al., 2004] have shown a transient decrease in Rad51 levels of approximately 70–80% in HeLa cells treated with Rad51C siRNA but not exposed to DNA damage (see Discussion). We note also that studies of the Rad51C defective hamster cell line irs3 show little effect on levels of Rad51 prior to DNA damage [French et al., 2002]. In that study there is still some Rad51 present in irs3 cells following DNA damage but it is unclear if a possible truncated form of Rad51C that may result from one of the exon 6 deleted transcripts still functions at some level to prevent loss of Rad51.

Western blots stained with either anti-Xrcc3 (Fig. 6B) or anti-Rad51C (Fig. 6C) again show specific loss of the RNAi-targeted protein. Additionally, while treatment of cells with Rad51 siRNA showed no decrease in the levels of either Xrcc3 or Rad51C (lane 2 in Fig. 6B,C), treatment with Rad51C siRNA resulted in a slight decrease in Xrcc3 (Fig. 6B, lane 4). On the other hand, treatment of cells with Xrcc3 siRNA resulted in an approximate 30% decrease in the level of Rad51C (Fig. 6C, lane 3). The extracts used in Figure 6B,C are from cells exposed to IR and very similar results are seen using cells not exposed to IR (not shown). However, Lio et al. [2004] have reported a more substantial loss of Xrcc3 in HeLa cells treated with Rad51C siRNAs but not exposed to DNA damage (see Discussion). Our data show that in no instance was the decrease in protein levels nearly as dramatic as that seen for Rad51 following treatment of cells with Rad51C

siRNA. Therefore, together with the immunofluorescence images in Figure 5, these data strongly support the idea that Rad51C serves to protect Rad51 against intracellular proteolysis, particularly following DNA damage.

Rad51C Protects Rad51 From Ubiquitin-Mediated Degradation that Is Enhanced Following DNA Damage

To investigate the mechanism of Rad51 degradation that occurs in the absence of Rad51C, we performed the following experiment using epoxomicin, a proteasome-specific inhibitor [Meng et al., 1999]. Cells treated with Rad51C siRNAs for 48 h were exposed to IR and incubated for an additional 2 h. One hour prior to IR treatment epoxomicin was added to a final concentration of 5 μM. Cells were harvested and Rad51 was immunoprecipitated. Controls included cells not exposed to IR, as well as mock epoxomicin treatment (DMSO alone in all—epoxomicin lanes in Fig. 7). The Western blots in Figure 7A were developed using mouse monoclonal anti-Rad51 and anti-mouse secondary antibodies, and therefore show the heavy and light chains of the monoclonal anti-Rad51 used for immunoprecipitation. Although these results reveal more Rad51 following IR exposure of Rad51C siRNA treated cells (Fig. 7A, lane 3) than the Western blot of whole cell extracts from similarly treated cells (Fig. 6A, lane 8), we note that epoxomicin results in an approximate three-fold increase in the level of Rad51 whether cells had been exposed to IR or not (Fig. 7A, lane 1 vs. 2, and lane 3 vs. 4). Therefore, inhibition of the proteasome clearly increases the steady state level of Rad51. These blots were stripped and re-probed with rabbit anti-ubiquitin and anti-rabbit secondary antibodies (Fig. 7B). Lanes 6 and 8 reveal a significant band of ubiquitinated Rad51 migrating at a position on the gel that approximates the molecular mass of Rad51 plus four ubiquitin chains. This number of Ub chains is suggested to be the minimum signal for targeting to the proteasome [Lam et al., 2002]. Cells not treated with Rad51C siRNA showed no detectable ubiquitinated-Rad51 in either the absence or presence of epoxomicin when not exposed to DNA damage (Fig. 7C, lanes 9 and 10). However, Ub-Rad51 is clearly present following exposure to IR when cells were treated with epoxomicin (compare Fig. 7C, lanes 11 and 12). Based on the total amount of protein loaded in each lane and scans of the Western blot, we estimate that the amount of Rad51-Ub trapped in the presence of epoxomicin is approximately two to three times greater in cells treated with Rad51C siRNA (Fig. 7B, lane 8) than in cells not treated with siRNA (Fig. 7C, lane 12). Therefore, while

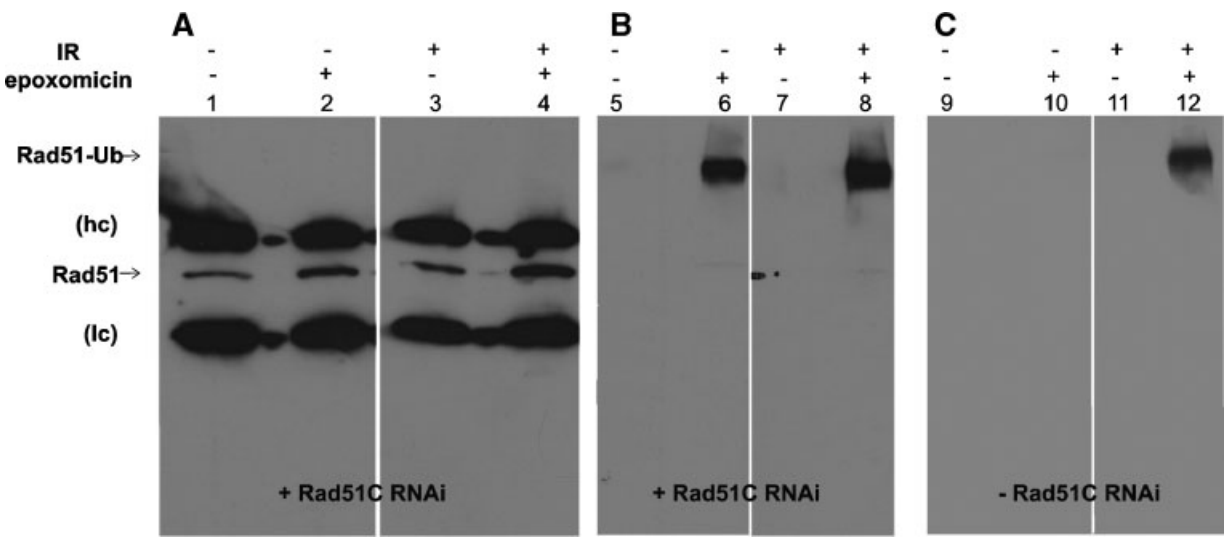

Fig. 7. Rad51C regulates ubiquitin-mediated proteasomal degradation of Rad51. **A**: Rad51 was immunoprecipitated from cells that had been treated with Rad51C siRNAs for 48 h and exposed to IR (0 or 8 Gy) in the absence or presence of epoxomicin. The blots were developed with the same antibody used for Rad51 immunoprecipitation, and the heavy and light chains of the monoclonal anti-Rad51 are indicated as (hc) and (lc), respectively. **B**: The blots in (A) were stripped and re-probed with anti-ubiquitin. **C**: HEK293 cells not treated with siRNA were processed exactly as those in **panel** (**A**) and the Western blot was probed with anti-ubiquitin.

it appears that ubiquitination and proteasomal degradation of Rad51 is a normal part of the DNA repair process, our data also reveal that Rad51C plays an integral role in regulating this effect.

DISCUSSION

The Rad51C and Xrcc3 proteins have been implicated as having important roles both early and late in the Rad51-catalyzed HR DNA repair pathway. In this study, we have focused on determining the cellular distribution of endogenous Rad51C and Xrcc3, as well as Rad51, over the course of IR-induced DNA damage and repair. As has been shown previously, we find that Rad51 forms discrete nuclear foci in response to DNA damage [Haaf et al., 1995; Bishop et al., 1998; Paull et al., 2000; Tashiro et al., 2000; Takata et al., 2001; Tarsounas et al., 2004]. We also show that these foci dissipate as DNA repair finishes, visualized by the disappearance of γH2AX foci. In contrast, we find that both Rad51C and Xrcc3 form discrete nuclear foci prior to DNA damage, and that these foci persist throughout the time course of DNA repair. It has been shown that formation of DNA damage-induced nuclear Rad51 foci requires the presence of each of the five Rad51 paralog proteins [Bishop et al., 1998; Takata et al., 2001] and that Xrcc3 nuclear foci form independently of Rad51 [Forget et al., 2004; this study]. We also show here that Rad51C nuclear foci form independently of Rad51. It may be, therefore, that the pre-damage nuclear Rad51C and Xrcc3 foci represent sites of protein function regarding their potential role in assisting the assembly of Rad51 nucleoprotein filaments at the sites of DNA breaks. We note that Rad51C and Xrcc3 can exist as a stable heterodimer [Kurumizaka et al., 2001; Masson et al., 2001a; Wiese et al., 2002], and that the relatively weak interaction between Rad51C and Rad51 is increased in the presence of Xrcc3 [Schild et al., 2000]. Alternatively, these foci may represent storage sites that release protein as needed during the DNA repair process. Further studies will be required to define the exact content and functional nature of these foci.

Our immunofluorescence images also show distinct staining for all three proteins in the cytoplasm and perinuclear region. Controls presented for antibody specificity using both Western blot and immunofluorescence methods, and the fact that both DAPI and γH2AX stains are localized exclusively to the nucleus, makes it unlikely that this results from artifacts in fixation or staining procedures. In fact, we note that other studies have reported a significant amount of Rad51 [Yoshikawa et al., 2000; Davies et al., 2001] and Rad51C [Miller et al., 2005] in the cytoplasm of human cells using Western blot analysis of sub-cellular fractions. It has been previously suggested that because Rad51C has a functional nuclear localization signal (NLS) it may serve as a transporter for those proteins with which it interacts but lack an NLS [French et al., 2003], Rad51 being one of those [Schild et al., 2000]. Partial localization of Rad51C at the perinuclear region is consistent with this idea. While studies of BRCA2 provide evidence for its direct participation in nuclear localization of Rad51 [Spain et al., 1999; Yuan et al., 1999; Davies et al., 2001; Godthelp et al., 2002; Tarsounas et al., 2004], further studies of Rad51C will be required to determine if it also contributes to the nuclear localization of Rad51 and related repair proteins in response to DNA damage.

Given that Rad51C and Xrcc3 form a stable heterodimer [Kurumizaka et al., 2001; Masson et al., 2001a; Wiese et al., 2002] and that Xrcc3 promotes the physical interaction of Rad51C and Rad51 [Schild et al., 2000], an important aspect of this work was to study the interdependence of the pattern of localization and the response to DNA damage for each protein. As expected, we observed that formation of DNA damage-induced Rad51 foci required the presence of Xrcc3. However, we have made the unexpected observation that RNAi-mediated knockdown of Rad51C leads to decreased levels of Rad51, and that this effect appears to be increased following DNA damage. Our data support the idea that in both cases, depletion of Rad51 results from ubiquitin-mediated proteasomal degradation because in the presence of epoxomicin, a proteasome-specific inhibitor, we observe the accumulation of ubquitinated-Rad51. The fact that the depletion of Rad51 and accumulation of epoxomicin-dependent Ub-Rad51 is significantly greater after cells have been exposed to IR suggests that this process is amplified by DNA damage. This is especially apparent in control cells not treated with any siRNAs. In this case we observe no Ub-Rad51 prior to DNA damage, and a level of Ub-Rad51 following DNA damage that is approximately

two to three fold less than in the absence of Rad51C. These results show that ubiquitination and degradation of Rad51 occur during the normal course of DNA repair, and that Rad51C plays an important role in regulating this process. This effect appears specific to Rad51C because RNAi-mediated knockdown of Xrcc3 does not diminish the level of Rad51 either before or after exposure of cells to DNA damage. Therefore, while a function for Rad51C in nuclear transport and/or loading of Rad51 onto a DNA break may be inferred from available genetic and cellular data, these new results identify a specific function for Rad51C in regulating Rad51 ubiquitination and degradation.

Other studies show that treatment of HeLa cells with Rad51C RNAi results in equivalent loss of both Rad51C and Xrcc3 that extends from 2 to 4 days post-RNAi transfection, while Rad51 levels shows a transient decrease at day 2 followed by recovery at day 3 [Lio et al., 2004]. In that study, cells were not exposed to DNA damage. In contrast, we see no significant decrease of Xrcc3 in cells treated with Rad51C RNAi whether or not cells had been exposed to DNA damage. Because we observed such a dramatic loss of Rad51 in cells treated with Rad51C RNAi that had subsequently been exposed to IR and very little effect of Xrcc3 knock down on Rad51 levels, we pursued studies of the mechanism of Rad51C regulation of Rad51 degradation. In ongoing work we are following a more detailed time course and IR dose dependence of the effect of loss of Rad51C and Xrcc3 on the ubiquitination and degradation of Rad51.

Earlier studies reported a non-covalent association of Ubl1 (SUMO 1) and Ubc9 (a SUMO E2 conjugating enzyme) with human Rad51 as demonstrated by yeast two-hybrid and co-immunoprecipitation experiments [Kovalenko et al., 1996; Shen et al., 1996a,b]. Additional studies have shown that in mink cells, treatment with TGFβ leads to ubiquitination and degradation of Rad51 [Kanamoto et al., 2002]. In yeast, both components of the 26S proteasome, the 19S regulatory cap and the 20S catalytic core, associate with an HO-induced DSB, and it has been suggested that the proteasome plays a role in DNA repair by clearing proteins following repair [Krogan et al., 2004]. The fact that we observe accumulation of Ub-Rad51 in normal HEK293 cells exposed to IR and treated with epoxomicin strongly suggests that proteasome-mediated clearing of DNA repair proteins also occurs in vertebrate cells. Our results also show that when Rad51C is removed from cells, Rad51 ubiquitination and degradation occurs both in the absence of DNA damage and to a greater extent following exposure of cells to IR. Therefore, this suggests that proteasome-mediated degradation plays a role in removing Rad51 from breaks following DNA repair and that Rad51C is involved in the regulation of this activity.

We note that BRCA1 has been shown to have E3 ubiquitin ligase activity [Lorick et al., 1999; Hashizume et al., 2001; Ruffner et al., 2001] but specific substrates have yet to be identified. If Rad51 is a BRCA1 E3 ligase substrate, it may be that Rad51C and BRCA1 compete for association with Rad51, and that following DNA repair, Rad51C is signaled to release Rad51 in favor of BRCA1, thereby resulting in ubiquitination and degradation of Rad51. With this link between the ubiquitin-mediated degradation pathway and Rad51C now established, it will be of great interest to study the relationship between the HR DNA repair proteins and components of the proteasome pathway to understand how activities are regulated to permit appropriate initiation, catalysis and termination of DSB repair.

ACKNOWLEDGMENTS

We are grateful for the technical support provided by Nick Willis, Robert Libfeld, Chris Bennett, and Dr. Elisabet Mandon. We thank Rachel Litman and Dr. Scott Young (Leica-Microsystems) for their support and critical comments on the work, Kate Lynott (Novus Biologicals) for her assistance, Dharia McGrew, and Annamaria Piermarini for help with the manuscript, and Genevieve Lo for her gracious support. B.T.B. is funded by a pre-doctoral fellowship from the D.O.D. Breast Cancer Research Program, and K.L.K. acknowledges support from NIH grants GM44772 and GM65851.

REFERENCES

Albala JS, Thelen MP, Prange C, Fan W, Christensen M, Thompson LH, Lennon GG. 1997. Identification of a novel human RAD51 homolog, RAD51B. Genomics 46: 476–479.

Aten JA, Stap J, Krawczyk PM, van Oven CH, Hoebe RA, Essers J, Kanaar R. 2004. Dynamics of DNA

double-strand breaks revealed by clustering of damaged chromosome domains. Science 303:92–95.

Bishop DK, Ear U, Bhattacharyya A, Calderone C, Beckett M, Weichselbaum RR, Shinohara A. 1998. Xrcc3 is required for assembly of Rad51 complexes in vivo. J Biol Chem 273:21482–21488.

Bleuyard JY, White CI. 2004. The Arabidopsis homologue of Xrcc3 plays an essential role in meiosis. EMBO J 23: 439–449.

Braybrooke JP, Spink KG, Thacker J, Hickson ID. 2000. The RAD51 family member, RAD51L3, is a DNA-stimulated ATPase that forms a complex with XRCC2. J Biol Chem 275:29100–29106.

Brenneman MA, Weiss AE, Nickoloff JA, Chen DJ. 2000. Xrcc3 is required for efficient repair of chromosome breaks by homologous recombination. Mutat Res 459: 89–97.

Cartwright R, Dunn AM, Simpson PJ, Tambini CE, Thacker J. 1998a. Isolation of novel human and mouse genes of the recA/RAD51 recombination-repair gene family. Nucleic Acids Res 26:1653–1659.

Cartwright R, Tambini CE, Simpson PJ, Thacker J. 1998b. The XRCC2 DNA repair gene from human and mouse encodes a novel member of the recA/RAD51 family. Nucleic Acids Res 26:3084–3089.

Chen F, Nastasi A, Shen Z, Brenneman M, Crissman H, Chen DJ. 1997. Cell cycle-dependent protein expression of mammalian homologs of yeast DNA double-strand break repair genes Rad51 and Rad52. Mutat Res 384: 205–211.

Chen J, Silver DP, Walpita D, Cantor SB, Gazdar AF, Tomlinson G, Couch FJ, Weber BL, Ashley T, Livingston DM, Scully R. 1998. Stable interaction between the products of the BRCA1 and BRCA2 tumor suppressor genes in mitotic and meiotic cells. Mol Cell 2:317–328.

Chen JJ, Silver D, Cantor S, Livingston DM, Scully R. 1999. BRCA1, BRCA2, and Rad51 operate in a common DNA damage response pathway. Cancer Res 59:1752s–1756s.

Daboussi F, Dumay A, Delacote F, Lopez BS. 2002. DNA double-strand break repair signalling: The case of RAD51 post-translational regulation. Cell Signal 14:969–975.

Davies AA, Masson JY, McIlwraith MJ, Stasiak AZ, Stasiak A, Venkitaraman AR, West SC. 2001. Role of BRCA2 in control of the RAD51 recombination and DNA repair protein. Mol Cell 7:273–282.

Dosanjh MK, Collins DW, Fan W, Lennon GG, Albala JS, Shen Z, Schild D. 1998. Isolation and characterization of RAD51C, a new human member of the RAD51 family of related genes. Nucleic Acids Res 26:1179–1184.

Forget AL, Bennett BT, Knight KL. 2004. Xrcc3 is recruited to DNA double strand breaks early and independent of Rad51. J Cell Biochem 93:429–436.

French CA, Masson JY, Griffin CS, O'Regan P, West SC, Thacker J. 2002. Role of mammalian RAD51L2 (RAD51C) in recombination and genetic stability. J Biol Chem 277:19322–19330.

French CA, Tambini CE, Thacker J. 2003. Identification of functional domains in the RAD51L2 (RAD51C) protein and its requirement for gene conversion. J Biol Chem 278:45445–45450.

Godthelp BC, Artwert F, Joenje H, Zdzienicka MZ. 2002. Impaired DNA damage-induced nuclear Rad51 foci formation uniquely characterizes Fanconi anemia group D1. Oncogene 21:5002–5005.

Haaf T, Golub EI, Reddy G, Radding CM, Ward DC. 1995. Nuclear foci of mammalian Rad51 recombination protein in somatic cells after DNA damage and its localization in synaptonemal complexes. Proc Natl Acad Sci USA 92: 2298–2302.

Haaf T, Raderschall E, Reddy G, Ward DC, Radding CM, Golub EI. 1999. Sequestration of mammalian Rad51-recombination protein into micronuclei. J Cell Biol 144: 11–20.

Hashizume R, Fukuda M, Maeda I, Nishikawa H, Oyake D, Yabuki Y, Ogata H, Ohta T. 2001. The RING heterodimer BRCA1-BARD1 is a ubiquitin ligase inactivated by a breast cancer-derived mutation. J Biol Chem 276:14537–14540.

Johnson RD, Jasin M. 2000. Sister chromatid gene conversion is a prominent double-strand break repair pathway in mammalian cells. EMBO J 19:3398–3407.

Kanamoto T, Hellman U, Heldin CH, Souchelnytskyi S. 2002. Functional proteomics of transforming growth factor-beta1-stimulated Mv1Lu epithelial cells: Rad51 as a target of TGFbeta1-dependent regulation of DNA repair. EMBO J 21:1219–1230.

Kovalenko OV, Plug AW, Haaf T, Gonda DK, Ashley T, Ward DC, Radding CM, Golub EI. 1996. Mammalian ubiquitin-conjugating enzyme Ubc9 interacts with Rad51 recombination protein and localizes in synaptonemal complexes. Proc Natl Acad Sci USA 93:2958–2963.

Krogan NJ, Lam MH, Fillingham J, Keogh MC, Gebbia M, Li J, Datta N, Cagney G, Buratowski S, Emili A, Greenblatt JF. 2004. Proteasome involvement in the repair of DNA double-strand breaks. Mol Cell 16:1027–1034.

Kurumizaka H, Ikawa S, Nakada M, Eda K, Kagawa W, Takata M, Takeda S, Yokoyama S, Shibata T. 2001. Homologous-pairing activity of the human DNA-repair proteins Xrcc3.Rad51C. Proc Natl Acad Sci USA 98: 5538–5543.

Lam YA, Lawson TG, Velayutham M, Zweier JL, Pickart CM. 2002. A proteasomal ATPase subunit recognizes the polyubiquitin degradation signal. Nature 416:763–767.

Lio YC, Schild D, Brenneman MA, Redpath JL, Chen DJ. 2004. Human Rad51C deficiency destabilizes XRCC3, impairs recombination, and radiosensitizes S/G2-phase cells. J Biol Chem 279:42313–42320.

Liu N, Lamerdin JE, Tebbs RS, Schild D, Tucker JD, Shen MR, Brookman KW, Siciliano MJ, Walter CA, Fan W, Narayana LS, Zhou ZQ, Adamson AW, Sorensen KJ, Chen DJ, Jones NJ, Thompson LH. 1998. XRCC2 and XRCC3, new human Rad51-family members, promote chromosome stability and protect against DNA cross-links and other damages. Mol Cell 1:783–793.

Liu N, Schild D, Thelen MP, Thompson LH. 2002. Involvement of Rad51C in two distinct protein complexes of Rad51 paralogs in human cells. Nucleic Acids Res 30: 1009–1015.

Liu Y, Masson JY, Shah R, O'Regan P, West SC. 2004. RAD51C is required for Holliday junction processing in mammalian cells. Science 303:243–246.

Lorick KL, Jensen JP, Fang S, Ong AM, Hatakeyama S, Weissman AM. 1999. RING fingers mediate ubiquitin-conjugating enzyme (E2)-dependent ubiquitination. Proc Natl Acad Sci USA 96:11364–11369.

Masson JY, Stasiak AZ, Stasiak A, Benson FE, West SC. 2001a. Complex formation by the human RAD51C and XRCC3 recombination repair proteins. Proc Natl Acad Sci USA 98:8440–8446.

Masson JY, Tarsounas MC, Stasiak AZ, Stasiak A, Shah R, McIlwraith MJ, Benson FE, West SC. 2001b. Identification and purification of two distinct complexes containing the five RAD51 paralogs. Genes Dev 15:3296–3307.

Meng L, Mohan R, Kwok BH, Elofsson M, Sin N, Crews CM. 1999. Epoxomicin, a potent and selective proteasome inhibitor, exhibits in vivo antiinflammatory activity. Proc Natl Acad Sci USA 96:10403–10408.

Miller KA, Yoshikawa DM, McConnell IR, Clark R, Schild D, Albala JS. 2002. RAD51C interacts with RAD51B and is central to a larger protein complex in vivo exclusive of RAD51. J Biol Chem 277:8406–8411.

Miller KA, Hinz JM, Yamada NA, Thompson LH, Albala JA. 2005. Nuclear localization of Rad51B is independent of Rad51C and BRCA2. Mutagenesis 20:57–63.

Paull TT, Rogakou EP, Yamazaki V, Kirchgessner CU, Gellert M, Bonner WM. 2000. A critical role for histone H2AX in recruitment of repair factors to nuclear foci after DNA damage. Curr Biol 10:886–895.

Pierce AJ, Johnson RD, Thompson LH, Jasin M. 1999. XRCC3 promotes homology-directed repair of DNA damage in mammalian cells. Genes Dev 13:2633–2638.

Rogakou EP, Pilch DR, Orr AH, Ivanova VS, Bonner WM. 1998. DNA double-stranded breaks induce histone H2AX phosphorylation on serine 139. J Biol Chem 273:5858–5868.

Ruffner H, Joazeiro CA, Hemmati D, Hunter T, Verma IM. 2001. Cancer-predisposing mutations within the RING domain of BRCA1: Loss of ubiquitin protein ligase activity and protection from radiation hypersensitivity. Proc Natl Acad Sci USA 98:5134–5139.

Schild D, Lio YC, Collins DW, Tsomondo T, Chen DJ. 2000. Evidence for simultaneous protein interactions between human Rad51 paralogs. J Biol Chem 275:16443–16449.

Shen Z, Pardington-Purtymun PE, Comeaux JC, Moyzis RK, Chen DJ. 1996a. Associations of UBE2I with RAD52, UBL1, p53, and RAD51 proteins in a yeast two-hybrid system. Genomics 37:183–186.

Shen Z, Pardington-Purtymun PE, Comeaux JC, Moyzis RK, Chen DJ. 1996b. UBL1, a human ubiquitin-like protein associating with human RAD51/RAD52 proteins. Genomics 36:271–279.

Sigurdsson S, Van Komen S, Bussen W, Schild D, Albala JS, Sung P. 2001. Mediator function of the human Rad51B-Rad51C complex in Rad51/RPA-catalyzed DNA strand exchange. Genes Dev 15:3308–3318.

Sonoda E, Takata M, Yamashita YM, Morrison C, Takeda S. 2001. Homologous DNA recombination in vertebrate cells. Proc Natl Acad Sci USA 98:8388–8394.

Spain BH, Larson CJ, Shihabuddin LS, Gage FH, Verma IM. 1999. Truncated BRCA2 is cytoplasmic: Implications for cancer-linked mutations. Proc Natl Acad Sci USA 96:13920–13925.

Sung P, Krejci L, Van Komen S, Sehorn MG. 2003. Rad51 recombinase and recombination mediators. J Biol Chem 278:42729–42732.

Takata M, Sasaki MS, Tachiiri S, Fukushima T, Sonoda E, Schild D, Thompson LH, Takeda S. 2001. Chromosome instability and defective recombinational repair in knockout mutants of the five Rad51 paralogs. Mol Cell Biol 21: 2858–2866.

Tambini CE, George AM, Rommens JM, Tsui LC, Scherer SW, Thacker J. 1997. The XRCC2 DNA repair gene: Identification of a positional candidate. Genomics 41:84–92.

Tarsounas M, Davies AA, West SC. 2004. RAD51 localization and activation following DNA damage. Philos Trans R Soc Lond B Biol Sci 359:87–93.

Tashiro S, Walter J, Shinohara A, Kamada N, Cremer T. 2000. Rad51 accumulation at sites of DNA damage and in postreplicative chromatin. J Cell Biol 150:283–291.

Tebbs RS, Zhao Y, Tucker JD, Scheerer JB, Siciliano MJ, Hwang M, Liu N, Legerski RJ, Thompson LH. 1995. Correction of chromosomal instability and sensitivity to diverse mutagens by a cloned cDNA of the XRCC3 DNA repair gene. Proc Natl Acad Sci USA 92:6354–6358.

Thacker J. 1999. A surfeit of RAD51-like genes? Trends Genet 15:166–168.

Thacker J. 2005. The RAD51 gene family, genetic instability and cancer. Cancer Lett 219:125–135.

Thompson LH, Schild D. 2001. Homologous recombinational repair of DNA ensures mammalian chromosome stability. Mutat Res 477:131–153.

West SC. 2003. Molecular views of recombination proteins and their control. Natl Rev Mol Cell Biol 4:435–445.

Wiese C, Collins DW, Albala JS, Thompson LH, Kronenberg A, Schild D. 2002. Interactions involving the Rad51 paralogs Rad51C and XRCC3 in human cells. Nucleic Acids Res 30:1001–1008.

Yoshihara T, Ishida M, Kinomura A, Katsura M, Tsuruga T, Tashiro S, Asahara T, Miyagawa K. 2004. XRCC3 deficiency results in a defect in recombination and increased endoreduplication in human cells. EMBO J 23:670–680.

Yoshikawa K, Ogawa T, Baer R, Hemmi H, Honda K, Yamauchi A, Inamoto T, Yazumi S, Motoda H, Kodama H, et al. 2000. Abnormal expression of BRCA1 and BRCA1-interactive DNA repair proteins in breast carcinomas. Int J Cancer 88:28–36.

Yuan SS, Lee SY, Chen G, Song M, Tomlinson GE, Lee EY. 1999. BRCA2 is required for ionizing radiation-induced assembly of Rad51 complex in vivo. Cancer Res 59:3547–3551.